Missing Energy and Jets for Supersymmetry Searches

Z. Bern[a], G. Diana[b], L. J. Dixon[c], F. Febres Cordero[d], S. Höche[c],

H. Ita[a,e], D. A. Kosower[b], D. Maître[f,g] and K. J. Ozeren[a]

[a] *Department of Physics and Astronomy, UCLA, Los Angeles, CA 90095-1547, USA*

[b] *Institut de Physique Théorique, CEA–Saclay, F–91191 Gif-sur-Yvette cedex, France*

[c] *SLAC National Accelerator Laboratory, Stanford University, Stanford, CA 94309, USA*

[d] *Departamento de Física, Universidad Simón Bolívar, Caracas 1080A, Venezuela*

[e] *Niels Bohr International Academy and Discovery Center, NBI, DK-2100, Copenhagen, Denmark*

[f] *Theory Division, Physics Department, CERN, CH–1211 Geneva 23, Switzerland*

[g] *Department of Physics, University of Durham, Durham DH1 3LE, UK*

Abstract

We extend our investigation of backgrounds to new physics signals, following CMS's data-driven search for supersymmetry at the LHC. The aim is to use different sets of cuts in $\gamma+$ 3-jet production to predict the irreducible $Z+$ 3-jet background (with the Z boson decaying to neutrinos) to searches with $\not{E}_T +$ 3-jet signal topologies. We compute ratios of $Z +$ 3-jet to $\gamma +$ 3-jet production cross sections and kinematic distributions at next-to-leading order (NLO) in α_s. We compare these ratios with those obtained using a parton shower matched to leading-order matrix elements (ME+PS). This study extends our previous work [1] on the $Z +$ 2-jet to $\gamma +$ 2-jet ratio. We find excellent agreement with the ratio determined from the earlier NLO results involving two instead of three jets, and agreement to within 10% between the NLO and ME+PS results for the ratios. We also examine the possibility of large QCD logarithms in these processes. Ratios of $Z+$ n-jet to $\gamma+$ n-jet cross sections are plausibly less sensitive to such corrections than the cross sections themselves. Their effect on estimates of $Z+$ 3-jet to $\gamma+$ 3-jet ratios can be assessed experimentally by measuring the $\gamma +$ 3-jet to $\gamma +$ 2-jet production ratio in search regions. We partially address the question of potentially large electroweak logarithms by computing the real-emission part of the electroweak corrections to the ratio using ME+PS, and find that it is 1% or less. Our estimate of the remaining theoretical uncertainties in the Z to γ ratio is in agreement with our earlier study.

I.   INTRODUCTION

The Large Hadron Collider has now produced more than two years of data from high-energy collisions. Data from the first year of running have been analyzed in a wide variety of searches, to seek new physics beyond the Standard Model, and to understand the underlying mechanism of electroweak symmetry-breaking. Search topologies with large missing transverse energy (MET) accompanied by several jets (METJ) play an important role in searches for supersymmetry and other models of new physics containing dark matter candidates.

Events with these topologies do not automatically point to new physics, as Standard-Model processes can give rise to similar ones. One example is the production of a Z boson in association with jets, with the Z then decaying into a pair of neutrinos (METZJ). METJ searches require that we understand these backgrounds.

The CMS collaboration has used [2, 3] W-boson and photon production in association with jets in order to estimate the METZJ background in setting limits on the constrained minimal supersymmetric standard model and on simplified models of new physics [4]. In such a data-driven approach, the unknown background is estimated by combining an experimental measurement of a reference process (which may be the same process in a different kinematic region) with a theoretical factor expressing the ratio between the two processes. This approach cancels the experimental systematics common to both processes, and can also reduce theoretical uncertainties. Theoretical input is still required to estimate the ratio and its uncertainties. The stability of the ratio under different theoretical approximations can be used to validate the theoretical uncertainty.

The most obvious choice of reference process to estimate the METZJ background would be another Z decay process, where the Z is again produced in association with jets, but decays to a charged-lepton pair. Only the Z branching ratio differs from the METZJ process. However, the rate for the charged-lepton process is a factor of six lower (per lepton flavor), even before taking into account reductions due to lepton rapidity cuts. The low statistics in the charged-lepton process has motivated experimenters to use other processes to estimate METZJ rates. The CMS collaboration has studied [2, 3] and used [4] W-boson or photon production in association with jets for making such estimates. The production of a W in association with jets offers an order of magnitude higher statistics than the leptonic Z process; the production of a prompt photon in association with jets, sixteenfold higher

statistics than leptonic Z decays. Photon production also avoids contamination from $t\bar{t}$ production. The cuts required to suppress this background in W production enhance the photon channel's advantage.

Photon production in association with jets has also been studied in ref. [5] and used by the ATLAS collaboration [6] in their data-driven estimates of the METZJ background. Another recent study has examined the scaling of $\gamma+$jets with the number of jets [7].

Both $W+$jets and $\gamma+$jets production probe different combinations of the parton distributions and different scales than $Z+$jets production. The impact of these effects must be determined theoretically. This in turn requires a theoretical study of ratios of photon production with respect to that of massive vector bosons.

The masslessness of the photon further requires a precise definition of what is meant experimentally by its detection. In the experiments, the photons must be isolated in order to eliminate otherwise-copious hadronic backgrounds, while overly strong isolation would lead to unwanted vetoing due to the underlying event. In a theoretical calculation, one must be careful to ensure that the photon-isolation criterion is infrared- and collinear-safe. Some QCD radiation must be allowed near the photon. This ensures that corresponding cross sections and distributions can be computed reliably in perturbation theory. Previous theoretical studies have used a variety of different isolation criteria, which are usually phrased in terms of the limits on the amount of hadronic energy in a cone surrounding the photon. Fixed isolation cones generally limit either the total amount of (transverse) energy in the cone, or the hadronic energy fraction of the total (transverse) energy in the cone. In contrast, the criterion proposed by Frixione [8] consists of a set of energy constraints that become increasingly restrictive the closer one gets to the photon. This latter criterion eliminates long-distance collinear fragmentation contributions of partons into photons. Its attractive theoretical properties flow from this fact. The other cone criteria require a perturbative factorization. While such a factorization is available, the required photon fragmentation functions [9] (non-perturbative functions analogous to the parton distribution functions) are not known very precisely.

In their study, CMS used [2, 3] a fixed hadronic-energy limit in an $R = 0.4$ cone surrounding the photon. In our previous study [1], we used a Frixione isolation criterion. In the same paper, we also showed that, at the large transverse boson momenta of interest in the search, the difference between the two isolation criteria was under 1%, a conclusion

confirmed by a comparison to an inclusive-photon measurement by CMS [10]. Additional jets are not expected to significantly alter this conclusion. As part of the present study, we have compared cross sections computed using a Frixione-type isolation with those imposing a standard-cone isolation for both $\gamma + 2$-jet and $\gamma + 3$-jet production, and find that the two are indeed within the expected 1% in the regions of interest. We used a parton shower matched to tree-level matrix elements (ME+PS) for this comparison. We will again use the Frixione isolation criterion in the present study.

Our previous study [1] looked at the $Z + 2$-jet and $\gamma + 2$-jet production processes at next-to-leading order (NLO) accuracy in the strong coupling α_s. We compared the NLO results with those computed using ME+PS. We provided the theoretical input needed for using the photon process to estimate the Z one, and for assessing the remaining theoretical uncertainties in this procedure. These results were used by the CMS collaboration to provide the theoretical uncertainty in their search for new physics based on topologies with large missing transverse energy and three or more jets [4].

In this article, we extend our study to $Z + 3$-jet and $\gamma + 3$-jet production at NLO in α_s. This is the first NLO computation of $\gamma + 3$-jet production at a hadron collider. In order to estimate the theoretical uncertainties on the ratios of the two processes, we will again compare the NLO results to the ME+PS ones. (The correlated variation of factorization and renormalization scales in the numerator and denominator of these ratios produces only small shifts in the ratios, which are likely to underestimate the uncertainties substantially.) We study these processes both with the selection cuts used by CMS [4] and studied for $\gamma + 2$-jet and $Z + 2$-jet production in ref. [1], and also with a set of tighter selection cuts. As we shall see, our results are consistent with our previous study, and indeed, the NLO ratios computed using $V + 3$-jet production are remarkably similar to those computed using $V + 2$-jet production, where V stands for both Z and γ.

The comparison of $V + 3$-jet to $V + 2$-jet production reveals potentially significant QCD logarithms, related to ratios of large scalar transverse energy and MET requirements to small minimum jet transverse momenta, which we examine. Liu *et al.* [11] have recently resummed a different class of logarithms (of threshold type) in $V + 2$-jet production processes. These are very similar to threshold logarithms previously resummed in pure QCD [12], and related to threshold logs resummed in top-quark production [13]. However, we are not aware of a comprehensive study of other large logarithms that may arise in such $V + n$-jet production

4

processes. At very large energies, virtual electroweak corrections are potentially significant, due to Sudakov double logarithms [14, 15]. As in ref. [1], we do not include these virtual effects. However, we have used the SHERPA parton-shower code to estimate the effects of radiating an additional real electroweak gauge boson, which decays hadronically. While this is not a detailed study, it suggests that the real-radiation effects are much smaller than those induced by virtual corrections [14, 15].

We employ the same software tools as in our previous studies of $W + n$-jet and $Z + n$-jet production [16–20]: the BLACKHAT library [21, 22] implementing on-shell methods numerically, along with AMEGIC++ [23] within the SHERPA [24] framework, to perform the leading-order (LO) and NLO calculations. We also use the SHERPA framework to obtain the ME+PS results. The public version of SHERPA does not properly treat the Z and γ cases on an equal footing, causing a bias as the number of jets increases. To obtain sensible predictions for the $Z + 3$-jet to $\gamma + 3$-jet ratio we have modified it somewhat.

This paper is organized as follows. In section II we outline our calculation. Section III discusses the various cuts we use. In section IV we present the total cross sections for $Z + 2$-jet, $Z + 3$-jet, $\gamma + 2$-jet and $\gamma + 3$-jet production for the different regions. In section V we examine jet production ratios (the ratio of $V + n$ jets to $V + (n-1)$ jets) in various regions of phase space. In section VI we present the ratios of $Z + 3$-jet to $\gamma + 3$-jet rates for cross sections, along with the corresponding ratios of $Z + 2$-jet to $\gamma + 2$-jet rates, and selected distributions. In section VII, we compare NLO QCD to ME+PS predictions and obtain an estimate of remaining theoretical uncertainties in the Z to γ ratio. We give our conclusions and outlook in section VIII. In the appendix we describe how we modified SHERPA so that Z bosons and photons are treated on an equal footing.

II. THE CALCULATION

We compute the cross sections at NLO in fixed-order perturbation theory, following the same basic organization as in previous studies [1, 16–18, 20]. We combine several contributions: the LO term; virtual corrections from the interference of tree-level and one-loop amplitudes; the real-emission corrections with dipole subtraction [25] terms; and the singular phase-space integrals of the dipole terms.

We evaluate the required one-loop amplitudes using the BLACKHAT program library [21],
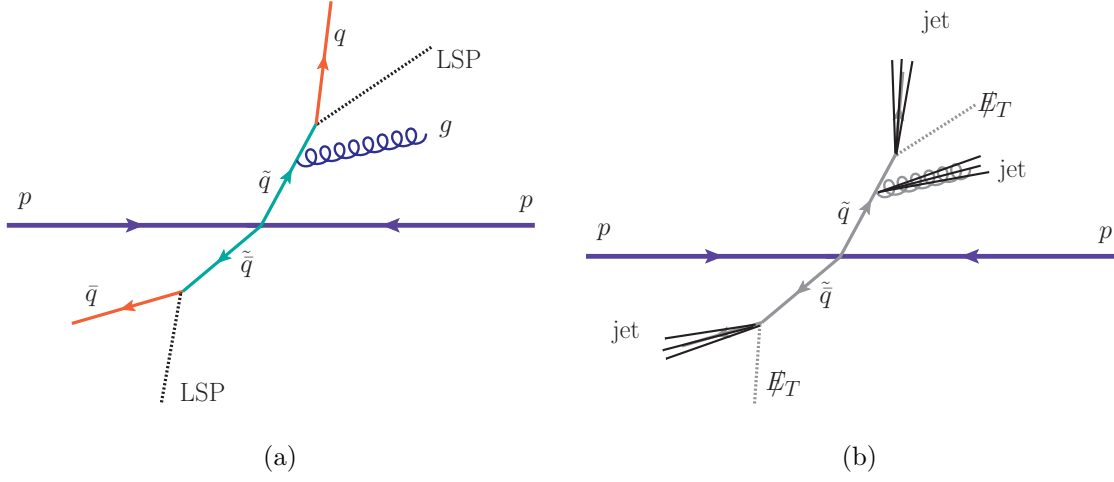
5

(a)   (b)

FIG. 1: Squark pair production illustrates a new-physics process with the signature of three jets plus MET. Here each squark decays to a quark and the lightest neutralino; the escaping neutralinos generate the missing transverse energy.
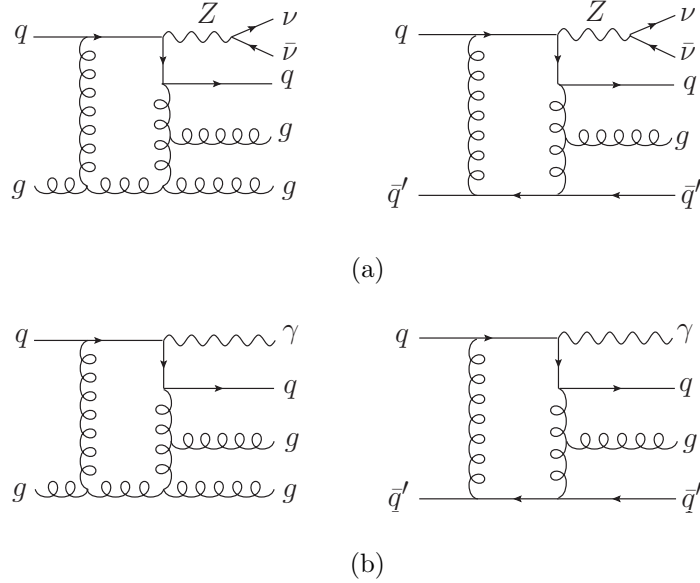

(a)

(b)

FIG. 2: Sample virtual diagrams needed for (a) $pp \to Z(\to \nu\bar{\nu}) + 3$-jet production and for (b) $pp \to \gamma + 3$-jet production.

which implements on-shell methods numerically. For the processes we are studying, we need the one-loop corrections to the following partonic processes,

$$q\bar{q}ggg \to Z(\to \nu\bar{\nu}) \text{ or } \gamma \,,$$
$$q\bar{q}q'\bar{q}'g \to Z(\to \nu\bar{\nu}) \text{ or } \gamma \,, \tag{2.1}$$

6

where three of the five partons are crossed into the final state, and the Z decay to neutrinos is folded in. We compute both distinct- and identical-quark flavor subprocesses for the second partonic process. We exhibit sample diagrams for these processes in fig. 2, illustrating the similarity of the Z and γ cases.

For both Z and γ processes, the BLACKHAT code library [21, 22] computes the required primitive amplitudes using a numerical implementation of on-shell methods. The photonic primitive amplitudes are obtained directly, rather than as sums over permutations of color-ordered primitive amplitudes for purely colored partons, as was done for the photonic amplitudes in our previous study [1]. We omit the process $gg \rightarrow ggg\gamma$ as it contributes to $\gamma + 3$-jet production only at $\mathcal{O}(\alpha_S^5)$, two orders higher than the LO processes in eq. (2.1). At the large values of parton x of interest here, the gluon luminosity is not large enough to compensate for the additional powers of α_s. As in refs. [18, 20], we drop small vector and axial loop contributions, along with the small effects of top quarks. However, all subleading color contributions are included. (See ref. [26] for a general method for doing so.)

The NLO result also requires real-emission corrections to the LO process, which arise from tree-level amplitudes with one additional parton. We use the AMEGIC++ code [23], included in the SHERPA framework, to compute these contributions, along with the Catani-Seymour dipole subtraction terms [25] and their integrals over phase space. We have previously validated [16, 18] the BLACKHAT+SHERPA framework for $W, Z + (n \leq 2)$ jets against the MCFM code [27].

In our study, we wish to vary the renormalization and factorization scales, and also to make use of parton distribution function (PDF) error sets to estimate associated uncertainties. To do so efficiently, we organize all contributions into sums of terms (in an automated way), where each term contains a simple function we wish to vary (for example, a logarithm of the renormalization scale) multiplied by a numerical coefficient independent of such variation. We calculate these coefficients in one run, and store them for re-use. For each event we generate, we record the momenta for all partons along with the coefficients of the various scale- or PDF-dependent functions. We store this information in ROOT-format n-tuple files [28]. The availability of these intermediate results in a standard format makes it straightforward for us to evaluate cross sections and distributions for different scales and PDF error sets. We can also furnish theoretical predictions to experimental collaborations by handing over n-tuple files. The experiments can modify the cuts applied, or compute

7

additional distributions [29–31].

We use the parton shower implemented in SHERPA to compute a parton-shower prediction matched to tree-level matrix elements (ME+PS), also known as matrix-element-plus-truncated-shower. The ME+PS event samples are produced following ref. [32], using the COMIX matrix-element generator [33]. (We expect the Z to γ ratios to be insensitive to hadronization effects; accordingly, to allow a cleaner comparison to the fixed-order NLO results, we do not include hadronization effects but present the ME+PS results at parton level.) However, as we explain in greater detail in the appendix, we do not use a standard public version of SHERPA. Instead we modify version 1.3.1, in order to ensure that low-scale radiation in $Z + n$-jet and $\gamma + n$-jet production is treated on the same footing.

We work to leading order in the electroweak coupling. The Z-boson couplings we use are given in ref. [18]. The $\nu\bar{\nu}$ invariant mass is distributed in a relativistic Breit-Wigner of width $\Gamma_Z = 2.49$ GeV about the Z boson mass of 91.1876 GeV. These values, along with $\alpha_{\rm QED}(M_Z) = 1/128.802$ and $\sin^2\theta_W = 0.230$, lead to a branching ratio for the neutrino mode in Z decay of $\mathrm{Br}(Z \to \nu\bar{\nu}) = 0.2007$. We use MSTW2008 LO and NLO parton distribution functions [34], with the QCD coupling α_s chosen appropriately in each case. Our results are for an LHC center-of-mass energy of 7 TeV. As explained in ref. [1] (see also refs. [35]), we use the zero-momentum-squared value, $\alpha_{\rm EM}(0) = 1/137.036$, for the electromagnetic coupling in the photon amplitudes.

Photon measurements make use of an isolation criterion. Experimental collaborations typically use a weighted isolation criterion (see *e.g.* ref. [2]), imposing a limit on the hadronic energy fraction in a cone around the photon, or simply on the total hadronic energy in the cone. The theoretical computation for this criterion requires the use of nonperturbative photon fragmentation functions. Frixione [8] proposed a modified isolation requirement which suppresses the collinear region of the phase space and thereby eliminates the need for a fragmentation-function contribution. We follow this proposal, requiring that the partons obey,

$$\sum_i E_{iT}\,\Theta\left(\delta - R_{i\gamma}\right) \le \mathcal{H}(\delta)\,, \tag{2.2}$$

for all $\delta \le \delta_0$, in a cone of fixed half-angle δ_0 around the photon axis. In this inequality, $R_{i\gamma}$ is the distance of parton i from the photon. The restricting function $\mathcal{H}(\delta)$ is chosen such that it vanishes as $\delta \to 0$ and thus suppresses collinear configurations, but allows soft

radiation arbitrarily close to the photon. We adopt

$$\mathcal{H}(\delta) = E_T^\gamma \, \epsilon \left(\frac{1 - \cos\delta}{1 - \cos\delta_0} \right)^n , \qquad (2.3)$$

where E_T^γ is the photon transverse energy.

As in our previous study of $Z + $ 2-jet and $\gamma + $ 2-jet production [1], we will use the Frixione cone, with $\epsilon = 0.025$, $\delta_0 = 0.3$ and $n = 2$. We studied the sensitivity to these parameters in ref. [1], and found it to be weak[1]. We also compared the predictions using these parameters to predictions made using standard-cone isolation of the isolated prompt-photon spectrum [10] measured by CMS. We found the differences between the Frixione and standard-cone isolation prescriptions to be relatively small, and less than 1% in the large-p_T^γ region that is our primary interest. We concluded that it was reasonable to use the Frixione isolation to model the Z to γ ratio in association with two jets for CMS's analysis, and that the same conclusion should hold for the Z to γ ratio in association with three jets. We have now used a ME+PS calculation to compare directly $\gamma + $ 3-jet production using Frixione isolation to a standard cone isolation mimicking CMS's criterion. This parton-shower calculation effectively includes only the perturbative contributions to the photon fragmentation function. Nonetheless, we again find that the two isolation criteria give very similar results in the high-p_T region, agreeing to within 1%, which buttresses our previous conclusion [1].

III. CONTROL AND SEARCH REGIONS

Our focus in this paper is on using distributions measured for inclusive $\gamma + $ 3-jet production to predict similar distributions assembled from inclusive missing $E_T + $ 3-jet events. We focus on two control regions and five search regions suggested to us by the CMS collaboration. One of these control regions and two of the search regions were used to set limits on supersymmetry and other new physics models, based on data collected in 2010 [4]. The other control and search regions, relevant for the much larger 2011 data set, apply harder

---

[1] We follow our previous study in the details of the jet algorithm: to obtain the cross section for $\gamma + m$ jets, we apply the jet-finding algorithm to all partons except the photon, whether inside the isolation cone or not. We insist that there be m jets lying outside the photon isolation cone that pass the jet rapidity and minimum-p_T cuts.

cuts which push out further on the tails of the underlying distributions. The different search regions are intended to be relevant in different regions of the parameter space of supersymmetric extensions to the Standard Model. We have generated a set of n-tuples, implementing the weakest of all the cuts we list below while generating events. The full cuts are applied during the analysis of n-tuple files.

We follow CMS and use the anti-k_T jet algorithm [36] with clustering parameter $R = 0.5$ throughout, where $R = \sqrt{(\Delta y)^2 + (\Delta \phi)^2}$ is the usual distance measure in terms of rapidity difference Δy and azimuthal angle difference $\Delta \phi$. Jets are ordered in p_T.

The CMS cuts make use of a special definition of the total transverse energy, which we label H_T^{jet}. It is the scalar sum of the transverse energies of all jets with $p_\mathrm{T} > 50$ GeV and pseudorapidity $|\eta| < 2.5$. We also define[2] a vector MET, as the negative of the sum of the transverse momenta of all jets with $p_\mathrm{T} > 30$ GeV and $|\eta| < 5$. Each region that we consider is distinguished by a different set of cuts on the quantities H_T^{jet} and $|\mathrm{MET}|$:

Set 1: $H_T^{\mathrm{jet}} > 300$ GeV, $|\mathrm{MET}| > 250$ GeV;

Set 2: $H_T^{\mathrm{jet}} > 500$ GeV, $|\mathrm{MET}| > 150$ GeV;

Set 3: $H_T^{\mathrm{jet}} > 300$ GeV, $|\mathrm{MET}| > 150$ GeV;

Set 4: $H_T^{\mathrm{jet}} > 350$ GeV, $|\mathrm{MET}| > 200$ GeV;

Set 5: $H_T^{\mathrm{jet}} > 500$ GeV, $|\mathrm{MET}| > 350$ GeV;

Set 6: $H_T^{\mathrm{jet}} > 800$ GeV, $|\mathrm{MET}| > 200$ GeV;

Set 7: $H_T^{\mathrm{jet}} > 800$ GeV, $|\mathrm{MET}| > 500$ GeV.

The cuts in Sets 1–3 are the same as those used by the CMS collaboration [4] and were also used in our previous study of $Z + 2$-jet and $\gamma + 2$-jet production. Sets 4–7 impose harder (tighter) cuts, appropriate for searches with larger data sets. In addition to computing the $Z + 3$-jet and $\gamma + 3$-jet cross sections, we repeat our previous 2-jet study, extending it to the new kinematic sets.

For all sets we require three jets with at least 50 GeV of transverse momentum and absolute pseudorapidity of at most 2.5. These jets are called 'tagging jets'. The azimuthal

---

[2] MET stands for 'Missing Transverse Energy', but in fact denotes the missing transverse momentum.

separation between the two leading tagging jets and the MET vector is required to satisfy $\Delta\phi(\text{MET}, \text{jet}_i) > 0.5$, $i = 1, 2$. We require that the jet with the third-highest p_T also be separated from the MET vector, $\Delta\phi(\text{MET}, \text{jet}_3) > 0.3$. Additional jets beyond the third are not subject to such a constraint. (When repeating the $V + 2$-jet study, obviously we require only two tagging jets, and the last constraint does not apply.)

In addition to the above cuts, for the $\gamma + 2, 3$-jet cross sections only, we impose photon isolation according to the Frixione [8] prescription, with parameters $\epsilon = 0.025$, $\delta_0 = 0.3$ and $n = 2$ in eq. (2.3). We also follow CMS and require a minimum R-space separation between the MET vector and each tagging jet of 0.4. The photon is required to have $|\eta| < 2.5$. We impose no explicit minimum p_T on the vector boson, although the MET cuts make it very likely to have large p_T.

The Set 1 cuts can be roughly characterized as the low-H_T^jet / high-MET region, whereas Set 2 is the converse, high-H_T^jet / low-MET. The reason for studying these two sets is that different SUSY production mechanisms are expected to lead to signals in different regions. Broadly speaking, Set 1 is geared towards catching direct squark decays, while Set 2 is designed for cascades with a W boson and a softer lightest supersymmetric particle (LSP). Set 3, which is inclusive of both the others, is a control region. Set 4 is again a control region, and is inclusive of the regions covered by Sets 5, 6, and 7. These sets push further into the tail of distributions, and are designed to search for heavier superpartners.

Our fixed-order results depend on the renormalization scale μ_R and factorization scale μ_F. These scales are unphysical, and hence physical cross sections should be independent of them; but a dependence on them necessarily appears when the perturbative series is truncated at a finite order. For fixed-order predictions, it is customary to estimate the uncertainty arising from omission of higher-order terms by varying these scales around some central value. The size of the resulting band is a useful diagnostic for those situations where fixed-order perturbation theory breaks down. The central value should be a typical hard scale in the process, to minimize the impact of potentially large logarithms. We choose the dynamical scale $\mu = \mu_R = \mu_F = H_T'/2$ for this central value, where H_T' is defined as the scalar transverse energy sum,

$$H_T' = \sum_i E_T^i + E_T(Z, \gamma) \,, \tag{3.1}$$

with i running over the partons and $E_T(V) \equiv \sqrt{M_V^2 + p_\text{T}^2}$. We evaluate cross sections at

11

five values of the common renormalization and factorization scale: $\mu/2, \mu/\sqrt{2}, \mu, \sqrt{2}\mu, 2\mu$. As we will discuss below, this procedure is expected to greatly underestimate uncertainties when applied to a ratio of cross sections with similar QCD properties.

IV. BASIC LHC PREDICTIONS

In this section we present total cross sections for the seven control and search regions defined in the previous section. We present results for $\gamma + 3$-jet and $Z + 3$-jet production at the LHC for $\sqrt{s} = 7$ TeV. We also update our previous results [1] for $\gamma + 2$-jet and $Z + 2$-jet production for the cuts of Sets 1–3, and extend them to Sets 4–7. In the $Z +$ 2-jet and $Z +$ 3-jet studies, we fold in the decay of the Z boson into neutrinos, which in turn give rise to missing transverse momentum. The branching ratio for the Z decay to neutrinos is largely responsible for the $\gamma +$ 3-jet cross section being about a factor of four to five larger than for $Z(\to \nu\bar{\nu}) + 3$ jets. The value of this ratio is the primary underlying motivation for our study, and is clearly visible in our tables and figures. In later sections, we will study various ratios constructed from the numbers presented here.

In table I, we display the total cross section for the different sets of cuts detailed in section III. For each set, we show three different theoretical predictions for the $Z +$ 3-jet and $\gamma +$ 3-jet cross sections in sequence: LO; ME+PS; and NLO. The final states in the fixed-order cases (LO and NLO) consist of the vector boson with the three tagging jets, and possibly an extra jet at NLO. In the parton-shower case, the final state can contain many jets, although virtual corrections are not taken into account. The ME+PS calculation is computed using SHERPA, modified from the public version 1.3.1 as explained in the appendix. The LO fixed-order predictions are the least reliable of the three and are shown only for reference purposes.

In all sets, the corrections from LO to NLO are modest at the central value of μ. The LO results are up to 9% larger. This is in sharp contrast to the $Z +$ 2-jet and $\gamma +$ 2-jet results presented in ref. [1], and recomputed here in table II, where the LO results are up to 34% lower. The larger corrections in $V +$ 2-jet production are expected, because the LO kinematics for $V +$ 2-jet production are more constrained than those for $V +$ 3-jet production, and they are relaxed considerably when going to NLO or ME+PS kinematics.

As in our earlier study, the ME+PS and NLO results again do not agree well for the Z

Set	Prediction	$Z + 3$-jet	$\gamma + 3$-jet
1	LO	$0.1996(0.0006)^{+0.1046}_{-0.0639}$	$0.856(0.002)^{+0.446}_{-0.273}$
	ME+PS	$0.157(0.001)$	$0.772(0.009)$
	NLO	$0.186(0.002)^{+0.007}_{-0.023}$	$0.830(0.007)^{+0.049}_{-0.109}$
2	LO	$0.1790(0.0005)^{+0.0946}_{-0.0576}$	$0.913(0.002)^{+0.479}_{-0.292}$
	ME+PS	$0.160(0.002)$	$0.844(0.009)$
	NLO	$0.170(0.002)^{+0.007}_{-0.022}$	$0.87(0.01)^{+0.04}_{-0.11}$
3	LO	$0.664(0.001)^{+0.346}_{-0.211}$	$3.461(0.006)^{+1.780}_{-1.090}$
	ME+PS	$0.533(0.006)$	$3.09(0.04)$
	NLO	$0.622(0.005)^{+0.022}_{-0.077}$	$3.25(0.03)^{+0.12}_{-0.40}$
4	LO	$0.2914(0.0007)^{+0.1529}_{-0.0933}$	$1.354(0.003)^{+0.704}_{-0.431}$
	ME+PS	$0.235(0.002)$	$1.21(0.01)$
	NLO	$0.270(0.003)^{+0.009}_{-0.033}$	$1.29(0.01)^{+0.07}_{-0.17}$
5	LO	$0.0341(0.0001)^{+0.0182}_{-0.0111}$	$0.1392(0.0004)^{+0.0741}_{-0.0450}$
	ME+PS	$0.0284(0.0003)$	$0.124(0.002)$
	NLO	$0.0319(0.0007)^{+0.0017}_{-0.0044}$	$0.132(0.001)^{+0.006}_{-0.017}$
6	LO	$0.0185(0.0001)^{+0.0099}_{-0.0060}$	$0.0839(0.0004)^{+0.0450}_{-0.0273}$
	ME+PS	$0.0173(0.0002)$	$0.079(0.001)$
	NLO	$0.0181(0.0003)^{+0.0015}_{-0.0026}$	$0.081(0.001)^{+0.006}_{-0.011}$
7	LO	$0.00275(0.00002)^{+0.00152}_{-0.00091}$	$0.01070(0.00005)^{+0.00588}_{-0.00354}$
	ME+PS	$0.00245(0.00003)$	$0.0100(0.0002)$
	NLO	$0.00267(0.00006)^{+0.00027}_{-0.00043}$	$0.0105(0.0002)^{+0.0008}_{-0.0016}$

TABLE I: Cross sections in pb for Z and γ production in association with three jets for the cuts of Sets 1–7 given in section III. The numbers in parentheses are Monte Carlo statistical errors, while the upper and lower limits represent scale dependence.

and γ cross sections separately. We do not expect the LO or ME+PS calculations to get the overall normalization correct. We will discuss the Z to γ ratios of these results in section VI.

The results for $Z + 2$-jet and $\gamma + 2$-jet production for Sets 1–3 differ slightly from our

Set	Prediction	Z + 2-jet	γ + 2-jet
1	LO	$0.5121(0.0005)^{+0.1878}_{-0.1276}$	$2.050(0.002)^{+0.745}_{-0.508}$
	ME+PS	$0.432(0.002)$	$1.93(0.02)$
	NLO	$0.546(0.002)^{+0.023}_{-0.050}$	$2.403(0.009)^{+0.204}_{-0.267}$
2	LO	$0.2002(0.0003)^{+0.0752}_{-0.0508}$	$0.933(0.001)^{+0.346}_{-0.235}$
	ME+PS	$0.236(0.002)$	$1.137(0.008)$
	NLO	$0.272(0.002)^{+0.038}_{-0.038}$	$1.351(0.006)^{+0.215}_{-0.201}$
3	LO	$1.234(0.001)^{+0.445}_{-0.304}$	$5.780(0.005)^{+2.050}_{-1.410}$
	ME+PS	$1.165(0.005)$	$6.12(0.04)$
	NLO	$1.445(0.005)^{+0.116}_{-0.156}$	$7.50(0.02)^{+0.89}_{-0.94}$
4	LO	$0.5091(0.0005)^{+0.1876}_{-0.1273}$	$2.179(0.002)^{+0.794}_{-0.540}$
	ME+PS	$0.486(0.002)$	$2.28(0.01)$
	NLO	$0.600(0.003)^{+0.051}_{-0.067}$	$2.797(0.006)^{+0.333}_{-0.357}$
5	LO	$0.0561(0.0001)^{+0.0217}_{-0.0146}$	$0.2179(0.0004)^{+0.0838}_{-0.0563}$
	ME+PS	$0.0544(0.0003)$	$0.228(0.003)$
	NLO	$0.0664(0.0004)^{+0.0061}_{-0.0079}$	$0.2695(0.0009)^{+0.0299}_{-0.0345}$
6	LO	$0.01696(0.00006)^{+0.00663}_{-0.00443}$	$0.0731(0.0002)^{+0.0285}_{-0.0191}$
	ME+PS	$0.0220(0.0002)$	$0.095(0.001)$
	NLO	$0.0245(0.0002)^{+0.0042}_{-0.0039}$	$0.1094(0.0006)^{+0.0196}_{-0.0177}$
7	LO	$0.00330(0.00001)^{+0.00136}_{-0.00089}$	$0.01274(0.00005)^{+0.00521}_{-0.00344}$
	ME+PS	$0.00377(0.00003)$	$0.0144(0.0001)$
	NLO	$0.00433(0.00004)^{+0.00062}_{-0.00064}$	$0.01696(0.00009)^{+0.00264}_{-0.00262}$

TABLE II: Cross sections in pb for Z and γ production in association with two jets for the cuts of Sets 1–7 given in section III. The numbers in parentheses are Monte Carlo statistical errors, while the upper and lower limits represent scale dependence.

previous results [1]. In the earlier study, we used six-flavor running of α_s, whereas here we use five-flavor running in order to be consistent with the parton distributions used. (Neither approach is completely theoretically consistent, because of the absence of a generated top-
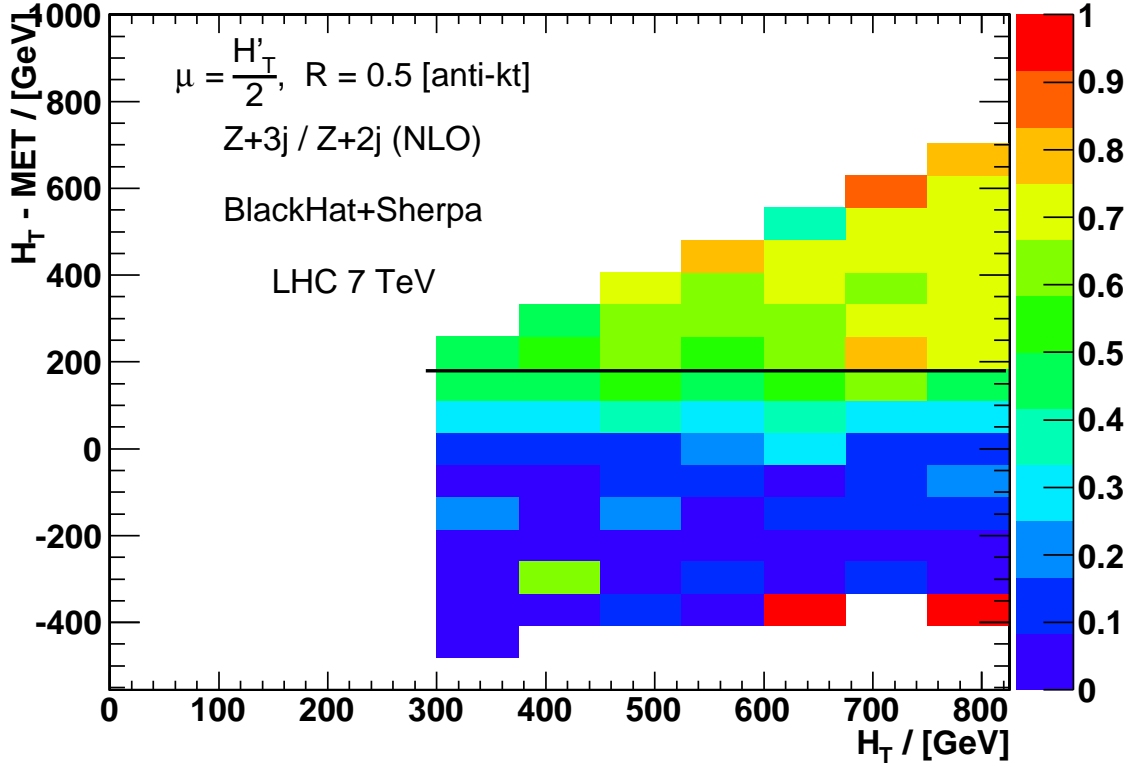
FIG. 3: The $Z + 3$-jet to $Z + 2$-jet ratio as a function of H_T^{jet} and $H_T^{\text{jet}} - |\text{MET}|$. The solid line shows where the ratio is roughly 0.5.

quark distribution.) With five-flavor running, the beta function is larger in magnitude, and hence $\alpha_s(\mu)$ decreases more rapidly above M_Z than with six-flavor running. Thus the $Z + 2$-jet production cross sections here are expected to be a bit smaller than those in ref. [1]. A naive estimate, based on the change in the value of α_s, suggests that 2% is the right magnitude of the difference, and this is indeed what we see in practice.

V. JET PRODUCTION RATIOS

The cuts presented in the previous section are quite different from typical cuts used to measure Standard-Model processes. They push the kinematic configurations far out onto tails of corresponding distributions. This introduces large ratios of scales, for example the ratio between H_T^{jet} and the minimum transverse momentum of a jet, p_T^{min}. Such large ratios can give rise to large logarithms. If sufficiently large, they may spoil the applicability of

Set	Prediction	$Z+$ 3-jet/$Z+$ 2-jet	$\gamma+$ 3-jet/$\gamma+$ 2-jet
1	LO	0.390(0.001)	0.418(0.001)
	ME+PS	0.364(0.004)	0.399(0.006)
	NLO	0.340(0.005)	0.346(0.003)
2	LO	0.894(0.003)	0.978(0.003)
	ME+PS	0.680(0.009)	0.74(0.01)
	NLO	0.625(0.008)	0.643(0.009)
3	LO	0.538(0.001)	0.599(0.001)
	ME+PS	0.458(0.006)	0.504(0.007)
	NLO	0.431(0.004)	0.433(0.004)
4	LO	0.572(0.001)	0.621(0.001)
	ME+PS	0.483(0.005)	0.532(0.006)
	NLO	0.450(0.005)	0.462(0.004)
5	LO	0.608(0.003)	0.639(0.002)
	ME+PS	0.523(0.006)	0.54(0.01)
	NLO	0.48(0.01)	0.490(0.005)
6	LO	1.088(0.008)	1.147(0.006)
	ME+PS	0.79(0.01)	0.84(0.01)
	NLO	0.74(0.01)	0.74(0.01)
7	LO	0.833(0.008)	0.840(0.005)
	ME+PS	0.649(0.009)	0.69(0.01)
	NLO	0.62(0.02)	0.62(0.01)

TABLE III: Ratios of cross sections for $Z+$ 3-jet to $Z+$ 2-jet and $\gamma+$ 3-jet to $\gamma+$ 2-jet for the cuts of Sets 1–7 given in section III. The numbers in parentheses are Monte Carlo statistical errors.

perturbation theory.

Before examining the results for the various sets of cuts presented in the previous section, let us explore the presence of large corrections which may be due to such logarithms. Our past studies [18] have shown that jet production ratios are convenient tools for this purpose.

We begin by examining the $Z + 3$-jet to $Z + 2$-jet and $\gamma + 3$-jet to $\gamma + 2$-jet ratios.

In table III, we show the values of these ratios for the different cut sets at LO, for the ME+PS calculation, and at NLO. At LO, the transverse momentum of the leading jet must be at least half the H_T^{jet} in $Z + 2$-jet or $\gamma + 2$-jet events; at NLO, this kinematic constraint is relaxed by real radiation. Accordingly, the LO distribution suffers large corrections in some regions. While an analogous kinematic relaxation does occur in $Z + 3$-jet and $\gamma + 3$-jet production when going from LO to NLO, the effect is much smaller. As a result, the $Z + 3$-jet to $Z + 2$-jet and $\gamma + 3$-jet to $\gamma + 2$-jet ratios suffer large NLO corrections for some ranges of H_T^{jet}; the LO values are typically 25–50% larger than the NLO ones.

We expect the NLO ratios to be more reliable, and focus on them. We show the $Z + 3$-jet to $Z + 2$-jet ratio in fig. 3 as a function of H_T^{jet} and $H_T^{\text{jet}} - |\text{MET}|$. The ratio depends much more strongly on $H_T^{\text{jet}} - |\text{MET}|$ than on H_T^{jet} alone. At LO, $H_T^{\text{jet}} - |\text{MET}|$ is necessarily positive, but the presence of additional radiation at NLO allows it to become negative.

When looser cuts typical of Standard-Model measurements are applied, with jet $p_{\text{T}} >$ 25 GeV, the $Z + 3$-jet to $Z + 2$-jet ratio is around 0.23 [20]. For jet $p_{\text{T}} > 30$ GeV, the ratio drops slightly to about 0.21, in agreement with the LHC data [29, 37]. In fig. 3, the darkest (blue) regions correspond to H_T^{jet} and $|\text{MET}|$ values for which the ratio is at most moderately enhanced above 0.21; lighter (green) areas, where the enhancement is noticeable, with a ratio around 0.5; and the lightest (yellow) areas, where the enhancement is significant, and the ratio approaches unity. At small or negative $H_T^{\text{jet}} - |\text{MET}|$, the ratio is only moderately enhanced. The enhancement grows with growing $H_T^{\text{jet}} - |\text{MET}|$, and is roughly independent of H_T^{jet} alone, when holding $H_T^{\text{jet}} - |\text{MET}|$ fixed. (The red squares at the bottom of the plot are Monte Carlo statistical fluctuations due to very small cross sections in this region.) The figure also shows a line corresponding roughly to a ratio of 0.5. We take this value to be the boundary between a region where the perturbative predictions are reliable, and a region where we cannot be as confident in them. Though our choice of boundary is arbitrary, it is motivated by the good agreement between theory and experiment for 3-jet to 2-jet ratios without vector bosons, up to a value of 0.5 [31]. We do not display the corresponding plot for the case where the Z boson is replaced by a photon; it is similar. It is plausible that, even in the region where the $Z + 3$-jet to $Z + 2$-jet ratio is above 0.5, large QCD enhancements will be independent of the parton distributions, and therefore will cancel in ratios such as the $Z + 3$-jet to $\gamma + 3$-jet ratio. However, we have no proof of the completeness

17

Set	$Z +$ 4-jet/$Z +$ 3-jet	$\gamma +$ 4-jet/$\gamma +$ 3-jet
1	0.233(0.004)	0.251(0.003)
2	0.451(0.013)	0.481(0.006)
3	0.260(0.006)	0.274(0.003)
4	0.287(0.010)	0.309(0.004)
5	0.341(0.011)	0.353(0.005)
6	0.616(0.021)	0.605(0.009)
7	0.464(0.027)	0.456(0.011)

TABLE IV: Ratios of LO cross sections for $Z +$ 4-jet to $Z +$ 3-jet and $\gamma +$ 4-jet to $\gamma +$ 3-jet for the cuts of Sets 1–7 given in section III. The numbers in parentheses are Monte Carlo statistical errors.

of this cancellation, and prefer to be conservative and acknowledge a lower reliability for the perturbative prediction in the region where the $V +$ 3-jet to $V +$ 2-jet ratio is larger than 0.5.

For Set 1, the NLO ratios are about 0.35; for Sets 3, 4, and 5, the ratios are larger but below 0.5; for the remaining Sets (2, 6, and 7), the ratios are bigger than 0.5 though still below 1. All these ratios are noticeably larger than the inclusive ratio with standard QCD measurement cuts [20, 29], for some sets larger by a substantial factor. For Set 1, it is not large enough to spoil the applicability of perturbation theory, and it is reasonable to assume this extends to Sets 3, 4, and 5. This assessment is reinforced by an examination of the $Z +$ 4-jet to $Z +$ 3-jet and $\gamma +$ 4-jet to $\gamma +$ 3-jet ratios at LO, shown in table IV. For Sets 2, 6, and 7, where the ratios are larger than 0.45, as discussed above one should be more cautious. Accordingly, our confidence in our uncertainty estimates for these sets is weaker, and would be weaker still for other, harder, search cuts. One cannot, of course, determine a precise value at which perturbation theory breaks down, but rather ranges where an investigation of potential logarithms and their resummation may be required. We note that the ME+PS predictions for the $V +$ 3-jet to $V +$ 2-jet production ratios, shown for comparison in table III, are typically between the NLO and LO results, and lie closer in value to NLO than to LO.

The $\gamma + n$-jet to $\gamma + (n\text{–}1)$-jet ratios discussed above can of course be measured experimentally. It would be interesting to do so for the search cuts listed above. This measurement, in

regions where one may question the applicability of unresummed QCD perturbation theory, could serve to increase our confidence in the use of purely perturbative tools to estimate QCD corrections to $Z + n$-jet to $\gamma + n$-jet ratios; or alternatively, to assess what additional corrections may be needed.

VI.   STABILITY OF THE Z TO γ RATIO

We turn next to a discussion of the target ratio, that between $Z + n$-jet and $\gamma + n$-jet production. In table V, we show the predicted ratio for each of the seven regions, based both on $V + 3$-jet production and on $V + 2$-jet production. The fixed-order predictions in the latter column are in good agreement with our previous study [1]. The last column shows the ratio of these predictions.

In the ratios, the LO scale variation cancels nearly completely, if we vary the scale identically in the $Z + 3$-jet and $\gamma + 3$-jet predictions, and correspondingly in the $Z + 2$-jet and $\gamma + 2$-jet predictions. In the NLO case the scale variation is a bit larger but also very small. Both scale variations lead to changes in the ratio of less than 0.5%. This nearly complete cancellation of the scale variation cannot be interpreted as a small theoretical uncertainty. We will instead use the closeness of the NLO and ME+PS ratios as an indication that the theoretical uncertainties for the individual cross sections do indeed largely cancel in the ratio. We account separately for the uncertainties due to the parton distributions. The Z to γ ratios depend mostly on the parton distributions through the $d(x)/u(x)$ ratio, and for regions of x where this quantity is relatively well measured. Hence the parton distribution uncertainties are small.

It is interesting that the NLO predictions for the Z to γ ratios in all sets are quite stable under the addition of a jet. That is, the predictions based on the ratio of $Z + 2$-jet to $\gamma + 2$-jet production are quite similar to those based on the $Z + 3$-jet to $\gamma + 3$-jet ratio. For the older sets (Sets 1–3), the predictions agree within 3%, and even for the newer sets (Sets 4–7), with harder cuts, the predictions agree to within 5%. The LO predictions differ by up to 10%, with the ME+PS results mostly in between in percentage difference. The NLO results should be used as the central values to which experimental measurements are compared.

We have also computed various distributions. Fig. 4 shows the LO, NLO, and ME+PS

Set	Prediction	$Z +$ 3-jet/$\gamma +$ 3-jet	$Z +$ 2-jet/$\gamma +$ 2-jet	ratio
	LO	0.2332(0.0008)	0.2499(0.0004)	0.933(0.004)
1	ME+PS	0.204(0.003)	0.224(0.002)	0.91(0.02)
	NLO	0.224(0.004)	0.227(0.001)	0.98(0.02)
	LO	0.1960(0.0007)	0.2145(0.0005)	0.914(0.004)
2	ME+PS	0.190(0.003)	0.207(0.002)	0.92(0.02)
	NLO	0.196(0.003)	0.201(0.001)	0.97(0.02)
	LO	0.1919(0.0005)	0.2134(0.0003)	0.899(0.003)
3	ME+PS	0.173(0.003)	0.190(0.001)	0.91(0.02)
	NLO	0.191(0.002)	0.1926(0.0008)	0.99(0.01)
	LO	0.2153(0.0007)	0.2336(0.0003)	0.922(0.003)
4	ME+PS	0.194(0.003)	0.213(0.002)	0.91(0.01)
	NLO	0.209(0.003)	0.215(0.001)	0.97(0.01)
	LO	0.245(0.001)	0.2574(0.0007)	0.952(0.005)
5	ME+PS	0.230(0.004)	0.239(0.004)	0.96(0.02)
	NLO	0.242(0.006)	0.246(0.002)	0.98(0.02)
	LO	0.220(0.002)	0.232(0.001)	0.948(0.008)
6	ME+PS	0.218(0.004)	0.232(0.003)	0.94(0.02)
	NLO	0.222(0.006)	0.224(0.002)	0.99(0.03)
	LO	0.257(0.003)	0.259(0.001)	0.99(0.01)
7	ME+PS	0.244(0.005)	0.261(0.003)	0.94(0.02)
	NLO	0.254(0.008)	0.255(0.003)	0.99(0.03)

TABLE V: Ratios of cross sections for $Z +$ 3-jet to $\gamma +$ 3-jet and $Z +$ 2-jet to $\gamma +$ 2-jet and their ratio for the cuts of Sets 1–7 given in section III. The numbers in parentheses are Monte Carlo statistical errors.

predictions for the H_T^{jet} distributions for all control and signal sets except Set 2 and 6 (which are subsets of Sets 3 and 4 respectively). The NLO and ME+PS predictions for the Z to γ ratio track each other well across the whole range of H_T^{jet}, although in Sets 3 and 5 the
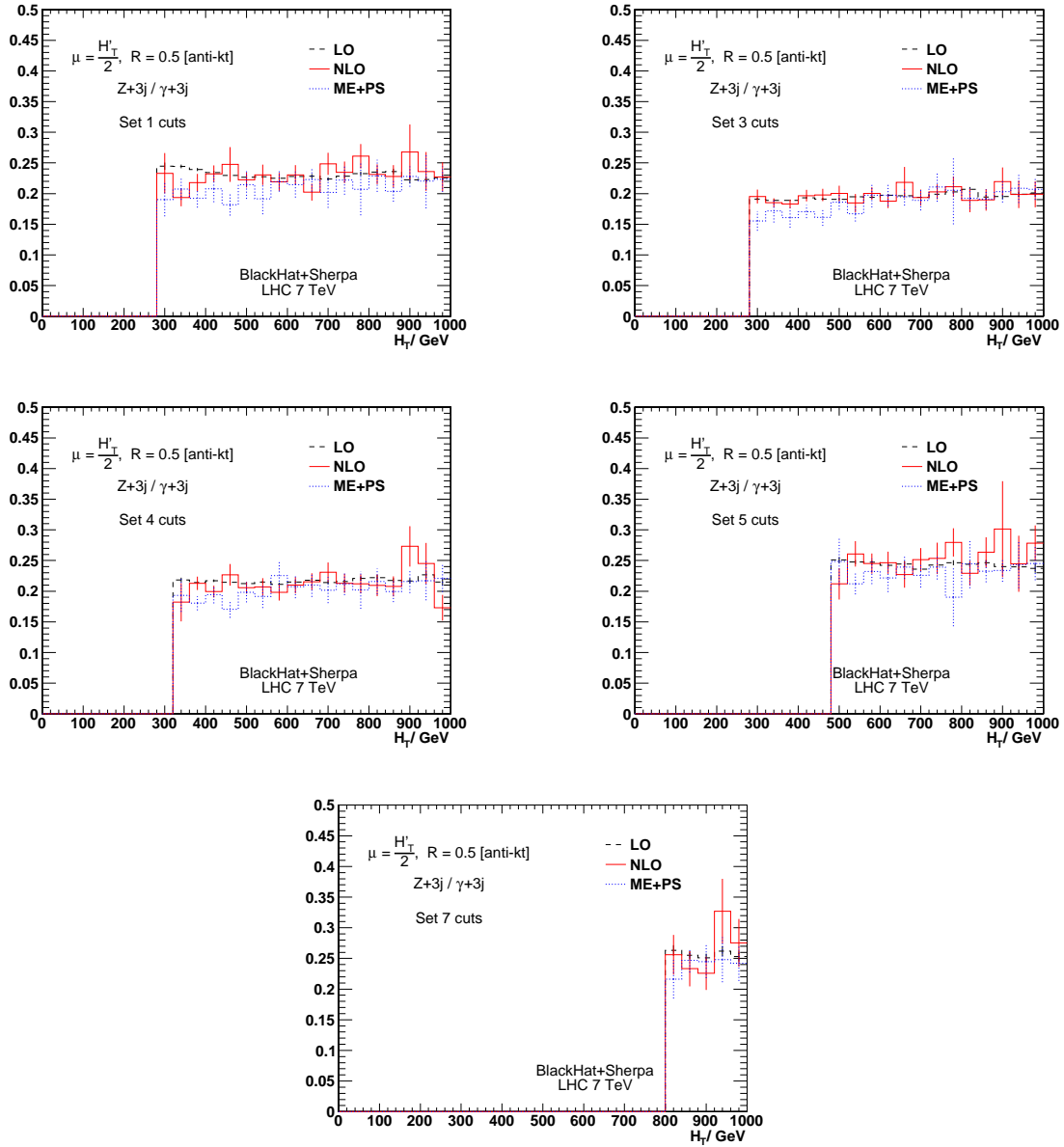
FIG. 4: The H_T^{jet} distribution for the ratio of $Z + 3$-jet to $\gamma + 3$-jet production for the different sets. We omit Sets 2 and 6, as these plots are subsets of those for Sets 3 and 4 respectively.

shapes of the distributions are somewhat different. (The total cross section in each set is of course dominated by the lowest bins above the minimum H_T^{jet}.)

The azimuthal angle $\Delta\phi(\text{MET}, \text{jet}_3)$ between the MET vector, which serves as a proxy for the vector-boson transverse momentum, and the softest jet is an interesting diagnostic of kinematic constraints on the jet. In fig. 5, we show the ratio of the distributions in $Z + 3$-jet production to that in $\gamma + 3$-jet production, for the cuts of Sets 1, 3, and 5. In all cases,

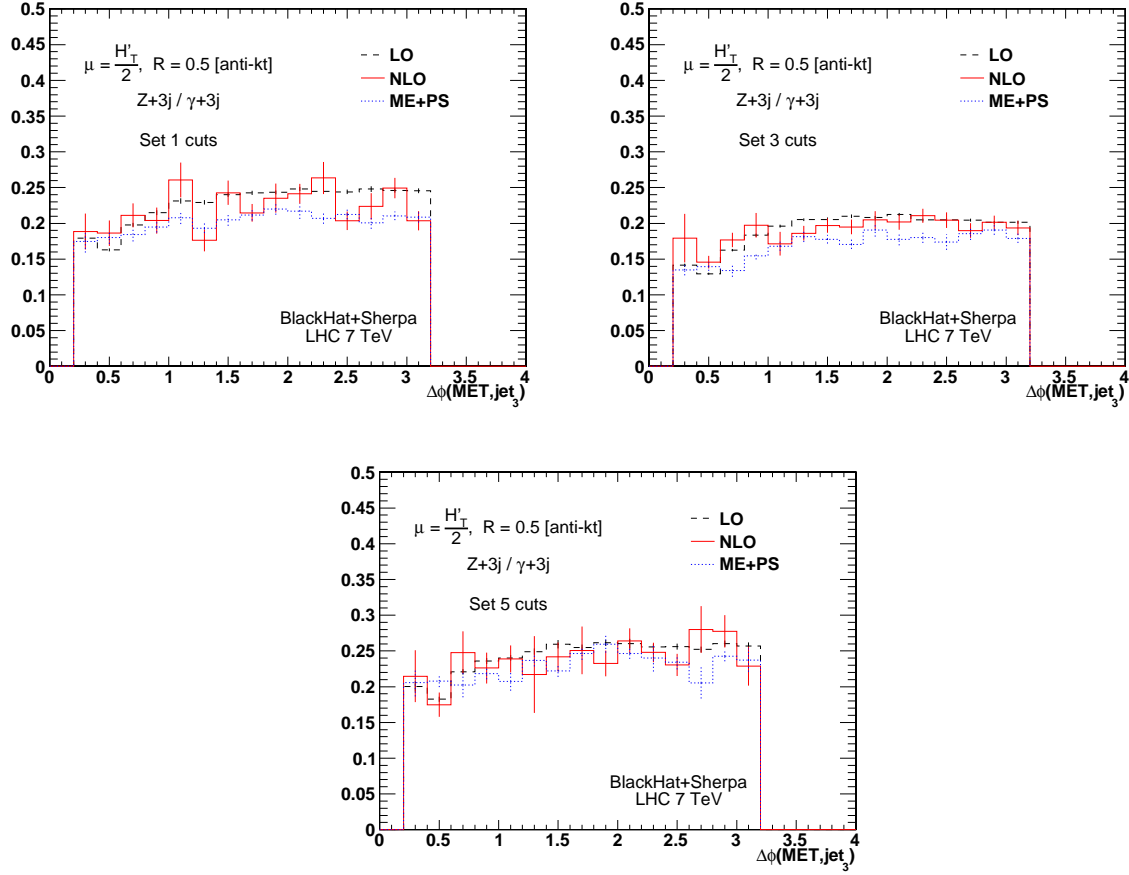FIG. 5: The ratio of the azimuthal angle distributions $\Delta\phi(\mathrm{MET}, \mathrm{jet}_3)$ in $Z + 3$-jet to $\gamma + 3$-jet production for sets 1, 3 and 5.

the ratio is fairly flat, with a slightly greater tendency in $Z + 3$-jet production compared to $\gamma + 3$-jet production for the softest jet to be on the opposite side of the event from the vector boson. Overall, the NLO corrections to the ratio are not large, at their largest staying below 15% in Set 1 at large $\Delta\phi$. In Set 5, all three approximations — LO, NLO, and ME+PS — are in reasonable agreement; in Set 3, the disagreements are not large but the NLO result is closer to the LO result than to the ME+PS one. In Set 1, the NLO suffers from large statistical errors, but appears to be roughly midway between the ME+PS and the LO results. The variability in the details of the comparison indicates that such details are indeed sensitive to the cuts and to the precise observable under examination. The overall reasonable agreement with LO is in sharp distinction to the comparison of the azimuthal angle between the MET vector and the second jet in $Z + 2$-jet and $\gamma + 2$-jet production [1], where the LO ratio differed markedly from both the NLO and ME+PS ratios, which were

22

Source \ Set	1	2	3	4	5	6	7
perturbative	0.09	0.03	0.10	0.07	0.05	0.02	0.04
PDF	0.02	0.03	0.02	0.02	0.03	0.04	0.05
photon-cone	0.01	0.01	0.01	0.01	0.01	0.01	0.01
total	0.09	0.04	0.10	0.08	0.06	0.04	0.06

TABLE VI: Estimates of the fractional uncertainty remaining from QCD effects for the $Z +$ 3-jet to $\gamma +$ 3-jet ratios. The "perturbative" uncertainty comes from comparing the NLO ratio with the ME+PS one, as explained in the text. The "photon-cone" uncertainty is due to the estimated difference in predictions using the standard and Frixione isolation cones.

in reasonable agreement with each other.

As noted earlier, we have used a modified version of SHERPA, based on version 1.3.1, in order to ensure that the competition of electroweak and QCD clusterings does not bias the Z to γ ratio. In the unmodified version, the biasing effect is substantial in the three-jet case, especially in the control regions (Sets 3 and 4).

VII. UNCERTAINTY ESTIMATES

A. QCD uncertainty

As discussed in section VI, the correlated scale variation in the NLO calculation largely cancels in ratios, and does not provide a suitable estimate of the remaining uncertainty due to uncomputed higher-order corrections. Instead, we use the NLO and ME+PS ratios presented in table V to evaluate the expected residual fractional uncertainty. For each set, we do this by dividing the absolute value of the difference between the two ratios by the NLO ratio. We add estimates of the PDF uncertainty, evaluated using MSTW08 68% error sets, and an estimate of the small uncertainty due to using the Frixione cone in the theoretical calculation of photon cross sections instead of the experimental fixed cone [1]. We treat the PDF uncertainties as uncorrelated in the numerator and denominator of the ratios, and combine them in quadrature. This somewhat overestimates this uncertainty, because they

Source \ Set	1	2	3	4	5	6	7
perturbative	0.02	0.03	0.01	0.00	0.03	0.03	0.02
PDF	0.02	0.03	0.02	0.02	0.03	0.03	0.05
photon-cone	0.01	0.01	0.01	0.01	0.01	0.01	0.01
total	0.03	0.04	0.02	0.02	0.04	0.05	0.05

TABLE VII: Uncertainty estimates for the $Z + 2$-jet to $\gamma + 2$-jet ratios. The labeling is as in table VI.

are in fact correlated; but this effect should be small, as the uncertainties are small. We also combine the three uncertainties in the table in quadrature to obtain the total uncertainty. The estimates based on inclusive $V + 3$-jet production are given in table VI, and those based on $V + 2$-jet production are given in table VII. One should be cautious in taking estimates smaller than 10% too literally, as the agreement between NLO and ME+PS may not reflect all missing contributions beyond that level. These uncertainty estimates should be taken symmetrically about the NLO $V + 3$-jet ratio as a central value. The overall uncertainty should be at the 10% level across all sets. This is in agreement with the estimate given in our earlier study [1]. For at least Sets 1–3, this theoretical uncertainty should be substantially smaller than other experimental uncertainties in CMS's supersymmetry limit [4].

B. A Partial Estimate of the Electroweak Uncertainty

At very large values of MET and H_T^{jet}, the effects of electroweak Sudakov logarithms are expected to become important [14, 15]. These effects arise from virtual exchanges of electroweak bosons between pairs of external partons or bosons that have large pair invariant masses, well above the vector-boson masses. In addition, one should expect corrections due to the real emission of electroweak gauge bosons from lower-jet multiplicity QCD processes, when the vector bosons decay to jets. A complete calculation of these corrections is beyond the scope of our present study. We can however, make crude estimates of the virtual corrections, along with a more reliable estimate of the leading real-emission corrections using ME+PS matched parton shower. For the latter purpose, we used the same modified version

Set	Z + 3-jet (real EW)	γ + 3-jet (real EW)	Z + 3-jet/γ + 3-jet (real EW)
1	0.0250(0.0003)	0.0162(0.0002)	0.0087(0.0002)
2	0.0169(0.0002)	0.0151(0.0002)	0.0017(0.0001)
3	0.0212(0.0003)	0.0140(0.0002)	0.0071(0.0002)
4	0.0221(0.0002)	0.0152(0.0002)	0.0068(0.0001)
5	0.0224(0.0003)	0.0183(0.0003)	0.0040(0.0001)
6	0.0139(0.0002)	0.0179(0.0003)	$-0.0040(0.0001)$
7	0.0208(0.0003)	0.0221(0.0005)	$-0.0012(0.0001)$

TABLE VIII: ME+PS predictions for fractional corrections to Z and γ production in association with three jets for the cuts of Sets 1–7 given in section III, where some of the jets may arise from the decay of an extra electroweak vector boson. The numbers in parentheses are Monte Carlo statistical errors.

of SHERPA as in section VI.

As a rough guide to the size of the electroweak virtual corrections, we can use fig. 7 of ref. [15]. This paper studies electroweak-boson production accompanied by a lone jet. For $|\text{MET}| \sim 250$ GeV, the effects in the Z to γ ratio will be under 5%; but for more aggressive cuts, $|\text{MET}| \sim 500$ GeV as in Set 7, they could grow to 10%. For higher MET cuts, the effects will grow beyond this value. This estimate does not take into account the additional jets, which for some subprocesses increase the number of electroweak radiators, and which also increase the partonic center-of-mass energy beyond that of the single-jet case. We expect MET to be more important than H_T^{jet} in determining the size of the virtual electroweak corrections to the Z to γ ratio, because the vector boson should have large invariant mass when paired with another parton, in order to give a different correction factor for a Z boson versus a photon.

The larger number of electroweak radiators in the processes of interest here may be expected to increase these effects somewhat, for a fixed value of $|\text{MET}|$, although a significant fraction of the cross section comes from subprocesses with a single quark line, which have the same number of electroweak radiators as in the calculation of ref. [15]. We expect these effects to increase the virtual contributions by 30% or so, say from a 10% correction to a 13% correction for $|\text{MET}| \sim 500$ GeV.

The virtual corrections are of course partially canceled by real emission of electroweak vector bosons [38]. The latter contribution can depend greatly on the observables and cuts. We expect the leading effect to be the emission of a W or Z boson from a configuration with two fewer jets, with the hadronic decay of the vector boson supplying the missing two jets. (If the vector boson is highly boosted, it might supply only a single merged jet.) We performed an ME+PS calculation, using SHERPA to generate matched matrix elements containing WZ, ZZ, $W\gamma$ and $Z\gamma$, along with up to two additional partons. The extra W or Z was then decayed hadronically, and the decay products were treated on an equal footing with the other jets in the event. In table VIII, we present the contribution of this additional vector boson emission to $Z + 3$ jets, to $\gamma + 3$ jets, and to the ratio, as a fraction of the basic calculation including only QCD emissions. While the effects of the electroweak real-emission contribution on the individual rates can exceed 2%, the corrections to the ratios are essentially negligible, 1% or less across all sets.

Overall, we believe that the net electroweak corrections, which are dominantly virtual, are likely to remain under 15%, even for Set 7. For even harder MET cuts, the effects may well become larger. A precise calculation of the one-loop electroweak effects, even just in leading or next-to-leading logarithmic accuracy, would clarify these questions.

VIII.   CONCLUSIONS AND OUTLOOK

In this paper, we have extended our previous study [1] of the theoretical issues encountered when using the measured $\gamma+$ jets signal to estimate the invisible $Z+$jets background in phase-space regions selected by strong cuts suitable for supersymmetry searches. In particular, we have provided an estimate of the remaining theoretical uncertainties in this translation. In the previous study, we used the $Z + 2$-jet to $\gamma + 2$-jet ratio in two search regions, along with a control region. These regions correspond to the sets used by the CMS collaboration in setting limits on supersymmetric partners from the 2010 LHC data [4]. In this paper, we have extended the study to an additional control region, and three new signal regions with stronger cuts. These new regions serve as a guide to searches with harder cuts, as appropriate for larger data sets. More importantly, we have added one more jet to the computation, letting us study the $Z + 3$-jet to $\gamma + 3$-jet ratio.

We computed the relevant differential cross sections and ratios to NLO in QCD, and

estimated the remaining perturbative QCD uncertainty to be 10% or less by comparing with a parton-shower calculation, matched to LO matrix elements (ME+PS), with the same number of jets. As explained in the appendix, we used a modified version of the SHERPA matching algorithm for this purpose. We also studied uncertainties due to the parton distribution functions, and found that they are 5% or less in the $Z + 2, 3$-jet to $\gamma + 2, 3$-jet ratios.

We used the Frixione isolation criterion to compute the prompt-photon cross sections. In our previous study, we compared isolated prompt-photon production with Frixione-cone isolation to that with fixed-cone isolation at NLO, and found that the resulting shift should be less than 1% in the high-p_{T}^{γ} region of interest. As part of our present study, we have compared $\gamma + 3$-jet production using a Frixione-cone and a fixed-cone in an ME+PS calculation; again we find a difference of less than 1% in the regions of interest.

Stronger cuts may also lead to larger QCD logarithms in the $V + 3$-jet to $V + 2$-jet ratios, which clouds our ability to rely on purely perturbative predictions. The smaller LO $V + 4$-jet to $V + 3$-jet ratios displayed in table IV suggest that this is not crippling; also, we may expect the large QCD corrections to mostly cancel in the $Z + 3$-jet to $\gamma + 3$-jet ratio. Experimenters could help part these clouds, and restore full confidence in the applicability of the perturbative uncertainty estimates in tables VI and VII, by measuring the ratio of $\gamma + 3$-jet to $\gamma + 2$-jet production in control and search regions, and comparing these to the theoretical predictions given in table III. We have not computed potentially-significant Sudakov logarithms arising from virtual electroweak corrections, but have given a crude estimate based on ref. [15]. We have computed the leading electroweak effects from emission of an additional W or Z, and find that these are 1% or less in the Z to γ ratio, fairly uniformly in all regions.

In summary, we find, across all search cuts, that the conversion between photons and Z bosons has less than a 10% theoretical uncertainty for events with either two or three associated jets. This is consistent with our previous findings [1]. These uncertainties are modest, and should make it possible for the photon channel to provide a competitive determination of the Standard-Model missing-E_T + jets background. Furthermore, the NLO predictions are remarkably robust under the addition of one jet, and should ideally be used as the central value for experimental comparisons.

Acknowledgements

Appendix A: Modification to SHERPA's ME+PS Algorithm

In this appendix we give a brief description of the ME+PS algorithm used in SHERPA, in order to explain how and why we modified the public version 1.3.1. The ME+PS method combines LO hard matrix elements together with parton showers, which resum logarithmic corrections due to gluon emission and parton splitting. The parton shower we use in SHERPA [39] is based on Catani-Seymour dipole factorization [25]. In contrast to earlier parton showers, the procedure inherently respects QCD soft color coherence. It allows the unambiguous identification of a recoil partner for partons that are shifted off their mass shell in the splitting process (the "mother" partons). This procedure eliminates one of the major sources of uncertainty in earlier schemes for parton evolution. We match the parton shower to matrix elements containing up to four final-state partons, and use 15 GeV for the merging cut. (Further details may be found in ref. [32].) When matching a parton shower to LO matrix elements using the CKKW algorithm [40], one must cluster back the matrix element configurations in order to define a parton-shower starting condition. In a shower that includes photons and electroweak gauge bosons, the clustering should include

the vectors as well [41].

Two issues arise. For the massive bosons, the reclustering is only done approximately, due to missing helicity information. This introduces a difference in the treatment of massive and massless electroweak gauge bosons, which affects the Z to γ ratio we are studying. We will not study this issue here. The other, and presumably more important, issue has to do with the ordering of clusterings involving the vector-boson decay products. There is no parton-shower equivalent to the $Z \to \nu\bar{\nu}$ decay, of course, but in reducing a full $Z + 3$- or $Z + 4$-parton final state to a lower-multiplicity parton initiator, the merging algorithm has to decide what to do with the neutrinos. (For hadronic Z decays there will be a full-fledged parton shower, and for Z decays to charged leptons additional QED radiation is possible.)

Ideally, the parton-shower history should factorize into two independent factors, one associated with Z production, and the other with Z decay. However, in SHERPA 1.3.1 the production and decay showers are interleaved. In particular, the neutrinos from Z decay are treated on an equal footing with the partons when creating the clustering history of an event (see sec. 4.4.2 of ref. [41]). The neutrinos are always produced with an invariant mass equal to the Z mass. Consequently, the treatment of radiation at scales below the Z mass differs between $Z + n$-jet and $\gamma + n$-jet production, affecting precisely the ratio we wish to compute. In more detail, the clusterings involving an electroweak object compete with the QCD clusterings, and the competition goes differently in the Z and γ cases. This creates a bias in the weighting of parton-shower initiators. The photon splitting amplitudes are simply color-stripped versions of the QCD ones, so the competition in the case of the photon gives the correct result. The bias shows up in ME+PS calculations of $Z + n$-jet production.

The effect turns out to be substantial in the high-p_{T} regions of interest in our study. Our modification to version 1.3.1 of SHERPA is simply to force the neutrino pair to cluster to a Z at the first CKKW step, and then to remove the associated scale from the cluster history. This modification guarantees that we treat the Z and photon identically in the ME+PS algorithm.

---

[1] Z. Bern, G. Diana, L. J. Dixon, F. Febres Cordero, S. Höche, H. Ita, D. A. Kosower and D. Maître, Phys. Rev. D **84**, 114002 (2011) [arXiv:1106.1423 [hep-ph]].

[2] CMS Collaboration, *"Data-Driven Estimation of the Invisible Z Background to the SUSY MET Plus Jets Search"*, CMS PAS SUS-08-002 (2008), unpublished.

[3] CMS Collaboration, *"Search for new Physics at CMS with Jets and Missing Momentum"*, CMS PAS SUS-10-005 (2010), unpublished.

[4] S. Chatrchyan *et al.* [CMS Collaboration], JHEP **1108**, 155 (2011) [arXiv:1106.4503 [hep-ex]].

[5] S. Ask, M. A. Parker, T. Sandoval, M. E. Shea and W. J. Stirling, JHEP **1110**, 058 (2011) [arXiv:1107.2803 [hep-ph]].

[6] G. Aad *et al.* [ATLAS Collaboration], Phys. Lett. B **710**, 67 (2012) [arXiv:1109.6572 [hep-ex]].

[7] C. Englert, T. Plehn, P. Schichtel and S. Schumann, JHEP **1202**, 030 (2012) [arXiv:1108.5473 [hep-ph]].

[8] S. Frixione, Phys. Lett. B **429**, 369 (1998) [hep-ph/9801442].

[9] L. Bourhis, M. Fontannaz and J. P. Guillet, Eur. Phys. J. C **2**, 529 (1998) [hep-ph/9704447].

[10] V. Khachatryan *et al.* [CMS Collaboration], Phys. Rev. Lett. **106**, 082001 (2011) [arXiv:1012.0799 [hep-ex]].

[11] X. Liu, S. Mantry and F. Petriello, Phys. Rev. D **86**, 074004 (2012) [arXiv:1205.4465 [hep-ph]].

[12] G. F. Sterman, Nucl. Phys. B **281**, 310 (1987);

S. Catani and L. Trentadue, Nucl. Phys. B **327**, 323 (1989);

N. Kidonakis, G. Oderda and G. F. Sterman, Nucl. Phys. B **525**, 299 (1998) [hep-ph/9801268];

N. Kidonakis, G. Oderda and G. F. Sterman, Nucl. Phys. B **531**, 365 (1998) [hep-ph/9803241];

E. Laenen, G. Oderda and G. F. Sterman, Phys. Lett. B **438**, 173 (1998) [hep-ph/9806467];

N. Kidonakis and J. F. Owens, Phys. Rev. D **63**, 054019 (2001) [hep-ph/0007268];

D. de Florian and W. Vogelsang, Phys. Rev. D **76**, 074031 (2007) [arXiv:0704.1677 [hep-ph]].

[13] E. Laenen, J. Smith and W. L. van Neerven, Nucl. Phys. B **369**, 543 (1992); Phys. Lett. B **321**, 254 (1994) [hep-ph/9310233];

E. L. Berger and H. Contopanagos, Phys. Lett. B **361**, 115 (1995) [hep-ph/9507363]; Phys. Rev. D **54**, 3085 (1996) [hep-ph/9603326];

S. Catani, M. L. Mangano, P. Nason and L. Trentadue, Phys. Lett. B **378**, 329 (1996) [hep-ph/9602208];

M. Czakon and A. Mitov, Phys. Lett. B **680**, 154 (2009) [arXiv:0812.0353 [hep-ph]];

V. Ahrens, A. Ferroglia, M. Neubert, B. D. Pecjak and L. L. Yang, JHEP **1009**, 097 (2010) [arXiv:1003.5827 [hep-ph]];

M. Beneke, P. Falgari, S. Klein and C. Schwinn, Nucl. Phys. B **855**, 695 (2012) [arXiv:1109.1536 [hep-ph]];

M. Cacciari, M. Czakon, M. L. Mangano, A. Mitov and P. Nason, Phys. Lett. B **710**, 612 (2012) [arXiv:1111.5869 [hep-ph]].

[14] E. Maina, S. Moretti and D. A. Ross, Phys. Lett. B **593**, 143 (2004) [Erratum-ibid. B **614**, 216 (2005)], [hep-ph/0403050].

[15] J. H. Kühn, A. Kulesza, S. Pozzorini and M. Schulze, JHEP **0603**, 059 (2006) [hep-ph/0508253].

[16] C. F. Berger, Z. Bern, L. J. Dixon, F. Febres Cordero, D. Forde, T. Gleisberg, H. Ita, D. A. Kosower and D. Maître, Phys. Rev. D **80**, 074036 (2009) [arXiv:0907.1984 [hep-ph]].

[17] C. F. Berger, Z. Bern, L. J. Dixon, F. Febres Cordero, D. Forde, T. Gleisberg, H. Ita, D. A. Kosower and D. Maître, Phys. Rev. Lett. **106**, 092001 (2011) [arXiv:1009.2338 [hep-ph]].

[18] C. F. Berger, Z. Bern, L. J. Dixon, F. Febres Cordero, D. Forde, T. Gleisberg, H. Ita, D. A. Kosower and D. Maître, Phys. Rev. D **82**, 074002 (2010) [arXiv:1004.1659 [hep-ph]].

[19] Z. Bern, G. Diana, L. J. Dixon, F. Febres Cordero, D. Forde, T. Gleisberg, S. Höche, H. Ita, D. A. Kosower, D. Maître and K. Ozeren, Phys. Rev. D **84**, 034008 (2011) [arXiv:1103.5445 [hep-ph]].

[20] H. Ita, Z. Bern, L. J. Dixon, F. Febres Cordero, D. A. Kosower and D. Maître, Phys. Rev. D **85**, 031501 (2012) [arXiv:1108.2229 [hep-ph]].

[21] C. F. Berger, Z. Bern, L. J. Dixon, F. Febres Cordero, D. Forde, H. Ita, D. A. Kosower and D. Maître, Phys. Rev. D **78**, 036003 (2008) [arXiv:0803.4180 [hep-ph]].

[22] C. F. Berger, Z. Bern, L. J. Dixon, F. Febres Cordero, D. Forde, T. Gleisberg, H. Ita, D. A. Kosower and D. Maître, Phys. Rev. Lett. **102**, 222001 (2009) [arXiv:0902.2760 [hep-ph]].

[23] F. Krauss, R. Kuhn and G. Soff, JHEP **0202**, 044 (2002) [hep-ph/0109036];

T. Gleisberg and F. Krauss, Eur. Phys. J. C **53**, 501 (2008) [arXiv:0709.2881 [hep-ph]].

[24] T. Gleisberg, S. Höche, F. Krauss, A. Schalicke, S. Schumann and J. C. Winter, JHEP **0402**, 056 (2004) [hep-ph/0311263];

T. Gleisberg, S. Höche, F. Krauss, M. Schönherr, S. Schumann, F. Siegert and J. Winter, JHEP **0902**, 007 (2009) [arXiv:0811.4622 [hep-ph]].

[25] S. Catani and M. H. Seymour, Nucl. Phys. B **485**, 291 (1997) [Erratum-ibid. B **510**, 503 (1998)] [hep-ph/9605323].

[26] H. Ita and K. Ozeren, JHEP **1202**, 118 (2012) [arXiv:1111.4193 [hep-ph]].

[27] J. M. Campbell and R. K. Ellis, Phys. Rev. D **65**, 113007 (2002) [hep-ph/0202176].

[28] R. Brun and F. Rademakers, Nucl. Instrum. Meth. A **389**, 81 (1997).

[29] G. Aad *et al.* [ATLAS Collaboration], Phys. Rev. D **85**, 032009 (2012) [arXiv:1111.2690 [hep-ex]].

[30] G. Aad *et al.* [ATLAS Collaboration], Phys. Rev. D **85**, 092002 (2012) [arXiv:1201.1276 [hep-ex]].

[31] Z. Bern, G. Diana, L. J. Dixon, F. Febres Cordero, S. Höche, D. A. Kosower, H. Ita, D. Maître, and K. Ozeren, Phys. Rev. Lett. **109**, 042001 (2012) [arXiv:1112.3940 [hep-ph]].

[32] S. Höche, S. Schumann and F. Siegert, Phys. Rev. D **81**, 034026 (2010) [arXiv:0912.3501 [hep-ph]].

[33] T. Gleisberg and S. Höche, JHEP **0812**, 039 (2008) [arXiv:0808.3674 [hep-ph]].

[34] A. D. Martin, W. J. Stirling, R. S. Thorne and G. Watt, Eur. Phys. J. C **63**, 189 (2009) [arXiv:0901.0002 [hep-ph]].

[35] B. A. Kniehl and L. Lönnblad, DESY 92–032 (1992), in *Proceedings of the Annecy Photon Workshop (1991)*;

A. Czarnecki and W. J. Marciano, Phys. Rev. Lett. **81**, 277 (1998) [hep-ph/9804252].

[36] M. Cacciari, G. P. Salam and G. Soyez, JHEP **0804**, 063 (2008) [arXiv:0802.1189 [hep-ph]].

[37] S. Chatrchyan *et al.* [CMS Collaboration], JHEP **1201**, 010 (2012) [arXiv:1110.3226 [hep-ex]].

[38] U. Baur, Phys. Rev. D **75**, 013005 (2007) [hep-ph/0611241].

[39] S. Schumann and F. Krauss, JHEP **0803**, 038 (2008) [arXiv:0709.1027 [hep-ph]].

[40] L. Lonnblad, JHEP **0205**, 046 (2002) [hep-ph/0112284];

S. Höche, F. Krauss, S. Schumann and F. Siegert, JHEP **0905**, 053 (2009) [arXiv:0903.1219 [hep-ph]].

[41] A. Schälicke and F. Krauss, JHEP **0507**, 018 (2005) [hep-ph/0503281].